

THE APPLICATION OF FINITE ELEMENT METHOD FOR DETERMINING THE THD IN THE ELECTROMOTIVE FORCE IN A SYNCHRONOUS MACHINE WITH PERMANENT MAGNETS UNDER DIFFERENT LOADS.

Plamen Rizov, Radoslav Spasov, Tsvetomir Stoyanov, Victor Zahariev

Abstract: In the report there is an algorithm given for determining the Total Harmonic Distortion (THD) in the electromotive force under different loads. Object of the study is a synchronous machines with excitation from permanent magnets imbedded in the rotor (SPMM), widely used in hybrid vehicles. There are two cases of stator windings studied – the first case is a three phase, ten pole machine with $q = 2$ (q - number of slots per pole and phase) and the second case is with two independent three phase, ten pole windings with $q = 1$. The study was made by modeling of the magnetic field with the “FEMM” software, and with additional program modules that calculate the THD in the software environment MatLab and Excel. As the obtained data is analyzed the value of the THD is compared to the previously determined standard values from previous studies and researches.

Keywords: Finite Element Method (FEM), Synchronous Permanent Magnet Motors, (SPMM), Total harmonic distortion (THD).

I. INTRODUCTION

The analyzed model is based on a widely used synchronous electrical motor that is used in modern hybrid cars and is constantly modified both in structure and used materials increasing its efficiency. There are many requirements towards these machines in terms of the power output to the weight of the machine, with the constant desire to increase power output and if possible decrease the vehicles weight.

Decreasing the weight of the machine is attained in several ways, but mostly by increasing the speed (turns per minute) and the current density in the windings by different means. Such methods are: using high energy permanent magnets (“rare earth magnets”), high grade insulation materials, special design of the sections of the stator windings (leading to a higher fill rate of the stator slots), using water or oils to directly cool the sections of the stator winding, using electrotechnical steel sheets with thickness from 0.35 mm to 0.15 mm and low eddy current losses.

From previously conducted studies [1] it is known that when using oil cooling the maximum current density in the stator windings is 30 A/mm^2 , which in term is allowing a significant improvement in the usage of the isolation system of the isolation system of the synchronous machine. In recent years the most common used electrical motors are those that have a V-shaped placement of the permanent

magnets on their rotors. In this type of configuration (Figure 1), two permanent magnets per pole are placed in a certain angle taking the form of a “V”. The main drawbacks of this design are the metal bridges that separate the permanent magnets from the air gap. There is a minimal thickness of the bridges that is fixed by mechanical constraints. This allows a large part of the permanent magnet flux to leak through these bridges instead of crossing the airgap and contributing to the torque.

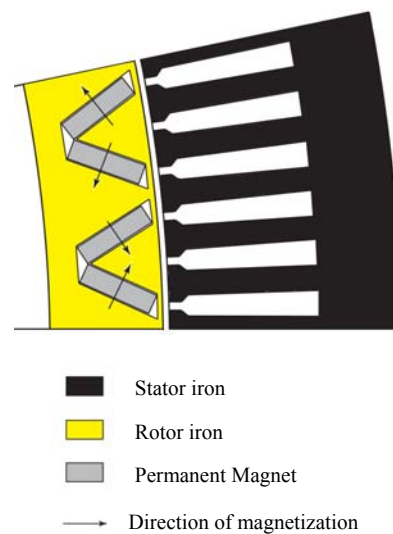


Figure 1. Cross-section of a V-shaped buried PM motor (one pole pair).

The stator section winding have a “hairpin” design and are made from rectangular conductors. These types of windings owe their exceptional efficiency because of their high slot fill rate (in contrast to conventional round wire windings). Multiple layers of interlocking “hairpin” windings conductors produce superior slot fill rates (up to 70 % versus 40% for the typical round wire winding). The design itself is patented and creates a shorter end turn space than other stator windings have, thereby reducing the stator temperature, increasing the motors torque, allows increasing the current density and leads itself to a stronger constriction at the critical connections between the conductors. These types of windings are well suited for liquid cooling which further enhances performance and reliability of the machine.

The characteristics and geometry of the machine are calculated and derived from previous studied models [2], [3] and are given in the following table (Table 1):

Case		1	2
Number of slots per pole and phase	-	q = 1	q = 2
Air gap	mm	0,7	0,7
Longitudinal length	mm	90	90
Stator outer diameter	mm	242	242
Stator inner diameter	mm	184,2	184,2
Number of stator slots	-	60	
Spatial angle between two slots in electrical degrees	deg	30	
Height of stator slots	mm	18,1	18,1
Width of stator slots	mm	5,8	5,8
Outer Rotor diameter	mm	182,8	182,8
Number of magnets in the Rotor	-	20	
Magnet material	-	NdFeB 40 MGOe	

Table 1. Machine characteristics

The winding type requires the usage of slots with parallel sides and stator teeth with varying width along the height. As the width of the stator teeth is not constant then the generated losses in them will vary with their height. This difference in losses will become more apparent with increasing the machines speed (increasing the frequency of the supplied voltage). The two windings studied are with a different number of

slots per pole and phase and have the same winding slot placement. In the machines with two sets of windings with different phase displacement of the current phase running in the first winding compared to the second. These two different cases of different winding slot placement (a different q) are shown in Figure 2 and Figure 3.

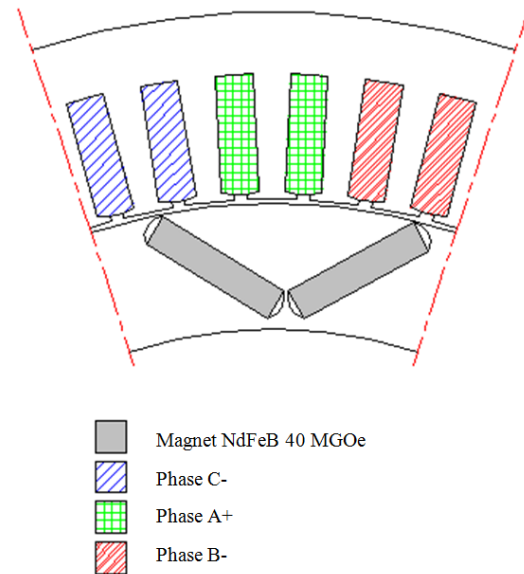


Figure 2. Cross-section of a stator windings machine with q = 2 (q - number of slots per pole and phase).

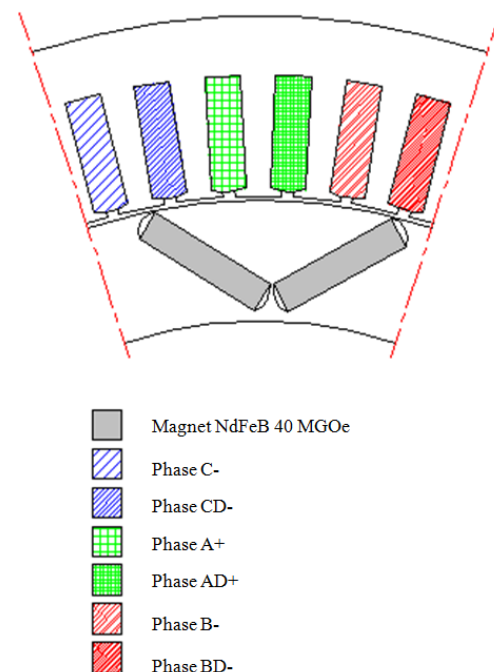


Figure 3. Cross-section of a stator windings machine with q = 1 (q - number of slots per pole and phase).

II. ANALYSIS

In the two studied models of windings the different input current values that are used the start point of phase displacement of the currents in time is the same. The start point in time is usually the moment the current in phase A has a maximum value and the currents in both phase B and phase C have values that are equal to half of their maximum values.

There are 3 different values for the stator current in each case studied. Each of the values for the stator current is equivalent to the following current densities in the stator slots: 10 [A/mm²], 20 [A/mm²], 30 [A/mm²]. For each current density the $\cos\varphi$ for that current varies from $\varphi=0.8$ to $\varphi=1$ for an inductive load and from $\varphi=0.8$ to $\varphi=1$ for a capacitive load. The shift from $\varphi=0.8$ to $\varphi=1$ as an inductive load and as well as for a capacitive load is made by a step of 0.05. For each different input current densities and $\cos\varphi$ the phase electromotive force is calculated forty times. The time interval between each calculation is set to interval of $t = 0.0005$ s that represents one turn of the machines rotor. The rotor spins clockwise with an angle of 1.8 degree (geometrical) that can be represented by 0.0005 seconds in the time line for each calculation.

The results of the electromotive force created at different load and power factor

($\cos\varphi$) for the first case main harmonic are displayed in Figure 4 and Figure 5. Figures 4 and Figure 5 display the electromotive force before any changes are made or simply depict case one from Table 1 where $q = 2$. Figures from Figure 6 up to Figure 11 show the electromotive force for harmonics two up to and including harmonic number twenty for different loads, and are divided into inductive and capacitive load ($\cos\varphi$). Due to the limitations of the current paper presentation volume the results of the electromotive force for any harmonic after number twenty won't be included.

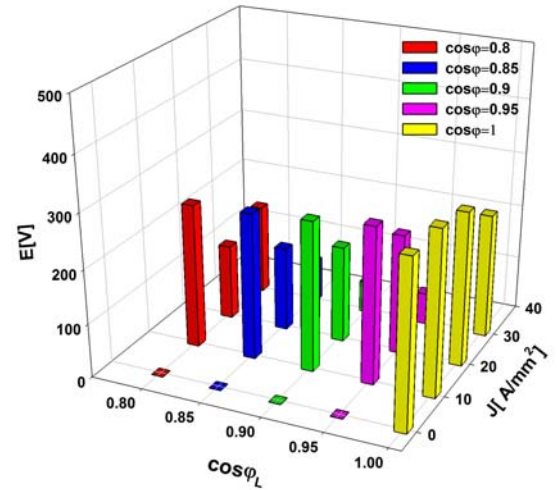


Figure 4. Main harmonic electromotive force at different currents densities and inductive $\cos\varphi$ values.

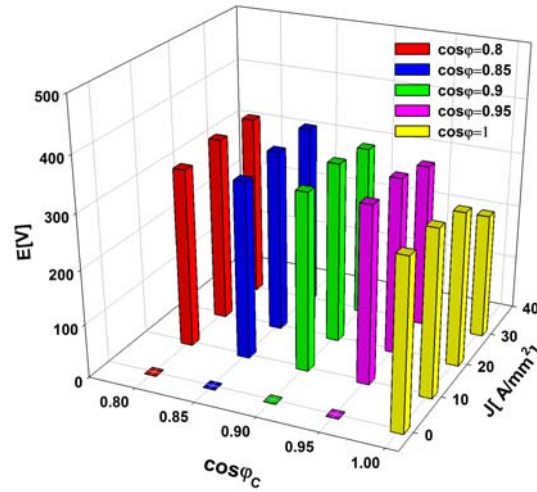


Figure 5. Main harmonic electromotive force at different currents densities and capacitive $\cos\varphi$ values.

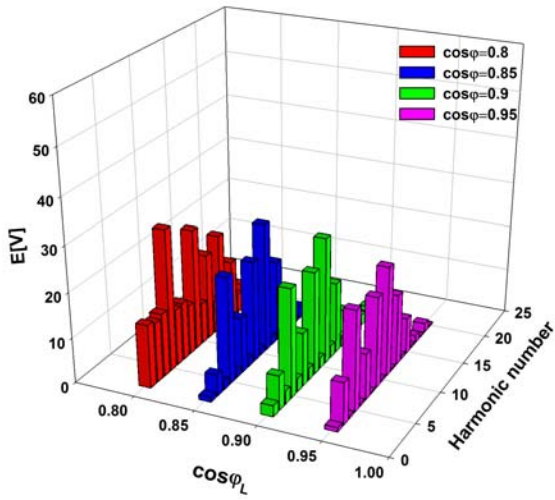


Figure 6. Electromotive force at 10 A/mm^2 current densities and inductive $\cos \phi$ values for the second to twentieth harmonic.

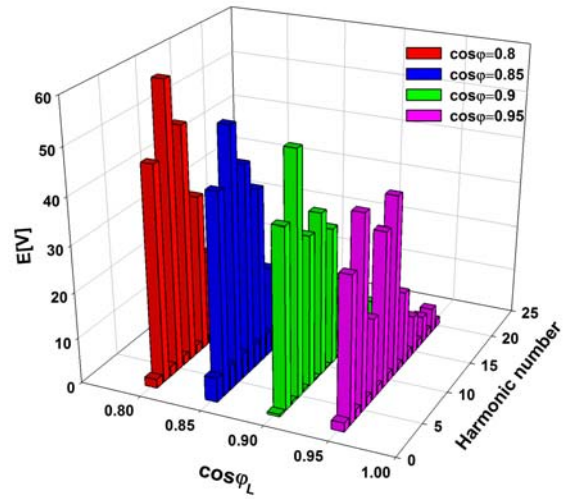


Figure 8. Electromotive force at 20 A/mm^2 current density and inductive $\cos \phi$ values for the second to twentieth harmonic.

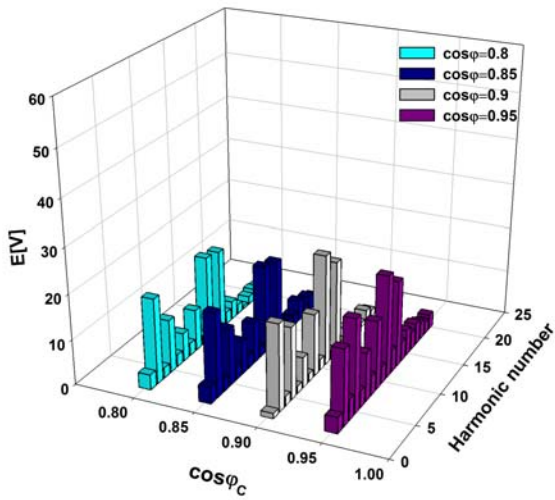


Figure 7. Electromotive force at 10 A/mm^2 current densities and capacitive $\cos \phi$ values for the second to twentieth harmonic.

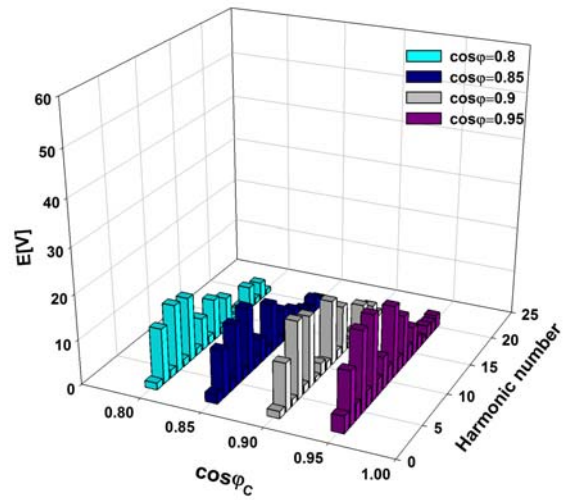


Figure 9. Electromotive force at 20 A/mm^2 current density and inductive $\cos \phi$ values for the second to twentieth harmonic.

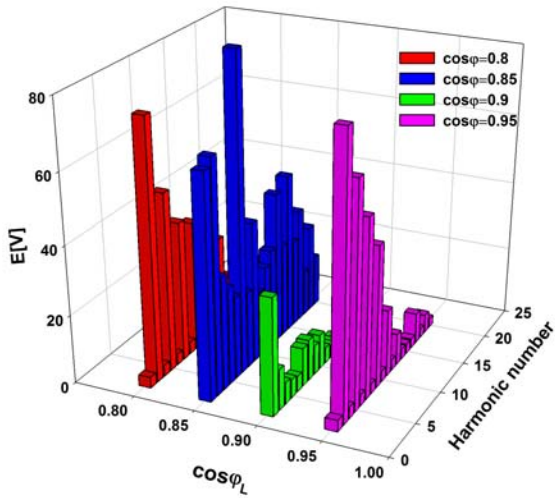


Figure 10. Electromotive force at 30 A/mm² current density and inductive cosφ values for the second to twentieth harmonic.

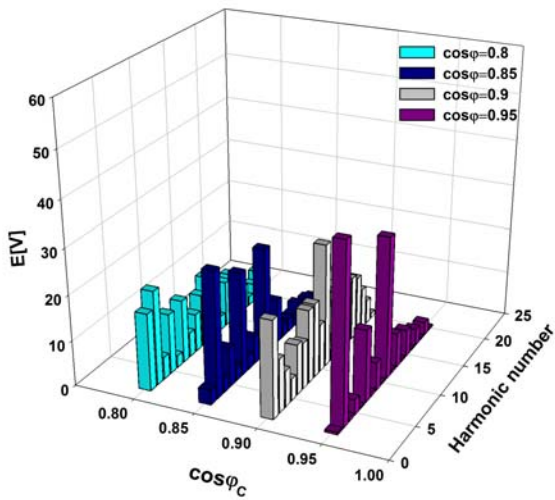


Figure 11. Electromotive force at 30 A/mm² current density and capacitive cosφ values for the second to twentieth harmonic.

As the received data for case two ($q = 1$) is analyzed it becomes apparent that when having low current density the results do not differ greatly when compared to case one ($q = 2$). When comparing case one and case two with a current density of 10 A/mm² it becomes apparent that the resulting electromagnetic force does not differ greatly they do not differ greatly.

When comparing the two cases of windings with a current density of 20 A/mm² and by studying different current phase displacement angles in the second winding compared to the first, in the second type of winding the total harmonic distortion (THD) greatly increases, which leads to an increase in the machine losses and a noticeable loss of electromotive force. And then as the load is increased to current densities of 30 A/mm² and a current phase displacement angle in the second winding is 30 degree, the total harmonic distortion decreases.

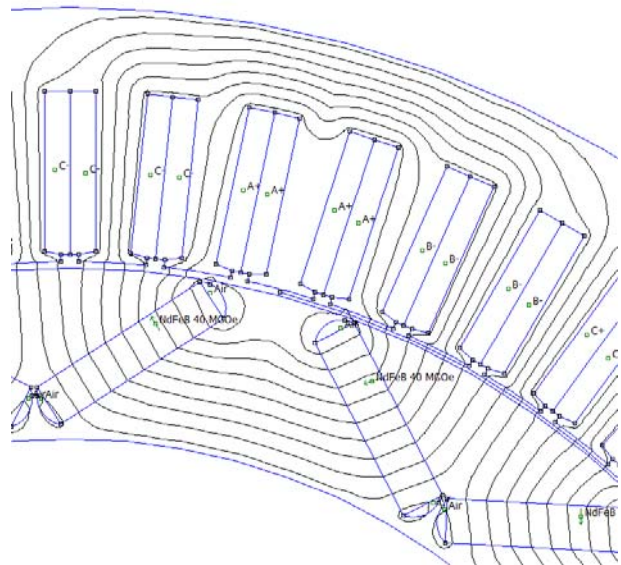


Figure 12. The flux line path of the electromagnetic field in the absence of a load.

The electromagnetic forces that were calculated and represented in the figures above can be used to create the machine's equations [5].

The flux distribution in both the rotor (Rt) and the stator (St) of the machine is illustrated in Figures 12 up to and including Figure 14.

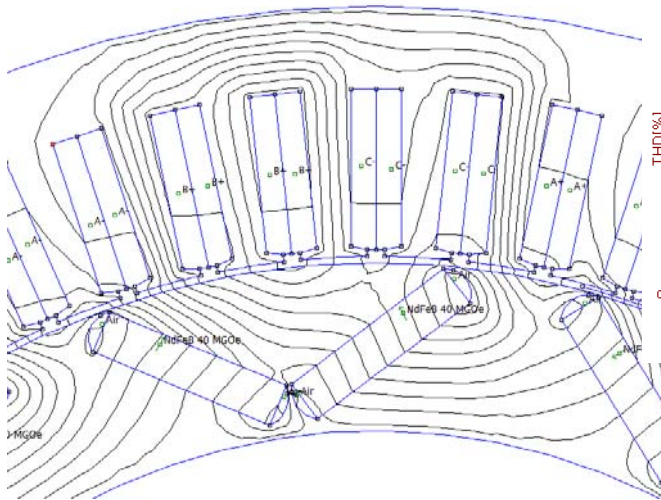


Figure 13. The flux line path of the electromagnetic field generated with a load of 30 A/mm^2 .

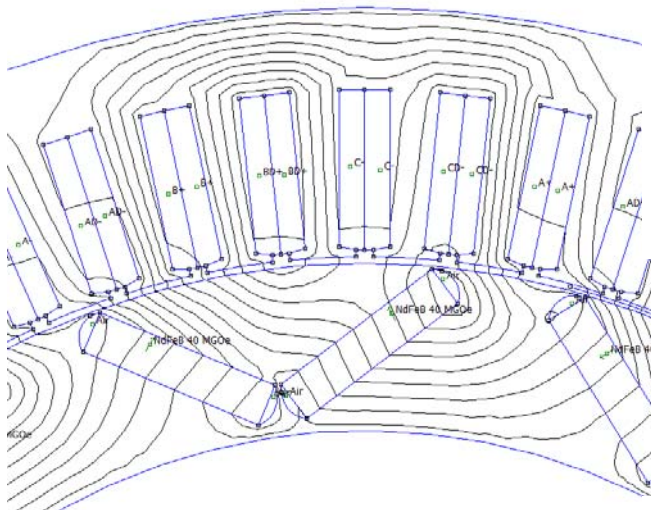


Figure 14. The flux line path of the electromagnetic field generated with a load of 30 A/mm^2 and a difference between the currents in two consecutive slots of 30 degree (electrical).

III. CONCLUSIONS

The base model or case one as given in Table 1 is used to study the effects of THD factor when using different stator windings while maintaining the machines geometry. This model allows the simulation and study of different input loads and phase placements.

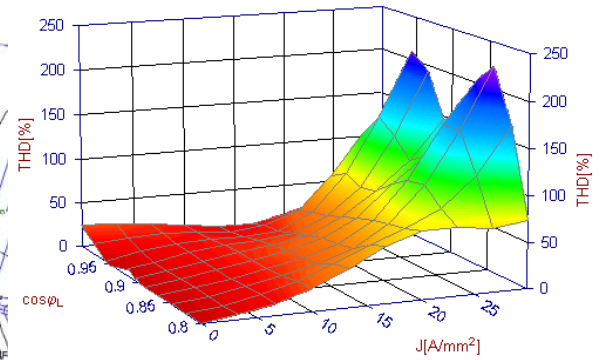


Figure 15. The total harmonic distortion at different current densities as the load is inductive.

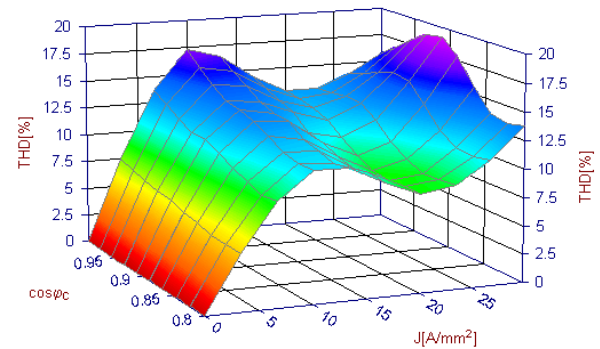


Figure 16. The total harmonic distortion at different current densities as the load is capacitive.

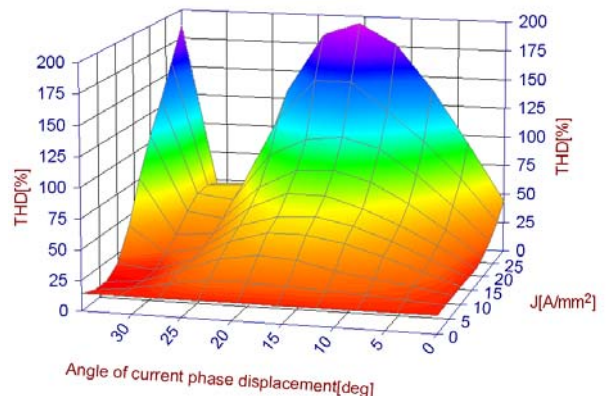


Figure 17. The total harmonic distortion at different current densities and current phase displacement angle.

Maintaining the optimal current phase angle between the second and the first winding is hard to achieve, because the phase shift unit needs to change its value according to the function of the load.

If the angle of phase displacement is different than the specified in the study that could lead to extremely high total harmonic distortion values.

In conclusion as the resulting electromotive force and THD factor are analyzed, case two is recommended for implementation in machines that are working continuously under large loads and not recommended in machines that work under varying load.

Tsvetomir Metodiev Stoyanov, department „Electrical Machines“, Technical University of Sofia, Kl. Ohridski Blvd 8, 1000, Sofia (SOF), Bulgaria, Block 12, lab 12314, Phone: +359 2 965-2453, e-mail: cecinh@abv.bg;

Victor Zahariev Zahariev, department „Electrical Machines“, Technical University of Sofia, Kl. Ohridski Blvd 8, 1000, Sofia (SOF), Bulgaria, Block 12, lab 12314, Phone: +359 2 965-2453, e-mail: sun_goko@gmail.com,

LITERATURE:

[1]. F. Libert, Royal Institute of Technology Department of Electrical Engineering Electrical Machines and Power Electronics, Stockholm 2004, Design, Optimization and Comparison of Permanent Magnet Motors for a Low-Speed Direct-Driven Mixer pp.7-24.

[2]. Ризов, П. , Р.Спасов, Ц. Стоянов, В. Захариев, Определяне на зависимостта на потокосцепленията от натоварването при синхронни машини с постоянни магнити за хибридни автомобили, Годишник на ТУ 2014.

[3]. Спасов, Р. , П. Ризов, В. Захариев, Ц. Стоянов, Приложение на метода на крайни елементи за определяне на момента и загубите в зъбите на статора при синхронни двигатели с вътрешни магнити, Годишник на ТУ 2014.

[4]. M. Varcaro N. Bianchi F. Magnussen, PM Motors for Hybrid Electric Vehicles The Open Fuels & Energy Science Journal, 2009, 2, 135-141.

[5]. Spasov V. An approach for coupling the field-circuit equations in the 3D voltage-fed finite element method with edge elements, Proceedings of the 10th International Conference on Electrical Machines, Drives and technologies “ELMA ‘2002”, Sofia, 13-14 September, Vol. I, 2002, pp. 192-199.

Contacts:

Plamen Milanov Rizov, department „Electrical Machines“, Technical University of Sofia, Kl. Ohridski Blvd 8, 1000, Sofia (SOF), Bulgaria, Block 12, lab 12329, Phone: +359 2 965-2147, e-mail: pmri@tu-sofia.bg;

Radoslav Lazarov Spasov, department „Electrical Machines“, Technical University of Sofia, Kl. Ohridski Blvd 8, 1000, Sofia (SOF), Bulgaria, Block 12, lab 12246, Phone: +359 2 965-2151, e-mail: rls@tu-sofia.bg;